

Fractal Nanotechnology

G. F. Cerofolini · D. Narducci · P. Amato ·
E. Romano

Received: 24 July 2008 / Accepted: 4 September 2008 / Published online: 23 September 2008
© to the authors 2008

Abstract Self-similar patterns are frequently observed in Nature. Their reproduction is possible on a length scale 10^2 – 10^5 nm with lithographic methods, but seems impossible on the nanometer length scale. It is shown that this goal may be achieved via a multiplicative variant of the multi-spacer patterning technology, in this way permitting the controlled preparation of fractal surfaces.

Keywords Spacer technology · Nanofabrication · Crossbar structure · Sub-lithographic preparation · Fractals

Introduction

Nanotechnology is essentially related to the problems of (1) predicting the properties of matter on the nanometer length scale, (2) preparing samples with accurately controlled size on that length scale, and (3) making accessible such samples to the macroscopic world. The first problem is essentially related to the fact that the nanoscale is characterized by the so called ($N + 1$) problem: the properties of a system with N particles may be largely different from those of a system with ($N + 1$) particles [1]. The preparation of nanoscopic samples with assigned properties requires therefore an extreme accuracy in the preparation.

The master road for the reproducible preparation of bodies in planar arrangement with assigned shape is photolithography. This technique has been able to produce features with progressively scaled size, the currently producible feature size being of several tens of nanometers. This size reduction, however, has been possible only thanks to the development of apparatuses of either huge economic cost (extreme ultraviolet lithography) or very low throughput (electron beam lithography).

In recent years, however, techniques not involving the use of advanced lithography have been developed for the preparation of nanometer-sized features. The most advanced ones are based on the transformation of vertical features into horizontal features and allow the preparation of lines with controlled width of 10–20 nm. Although this strategy allows the preparation of simple geometries only (line arrays), the development of new architectures [2] makes up for this inherent limitation. Among them the crossbar structure is particularly attractive [3, 4, 5] because it may simply be produced by crossing two perpendicularly oriented wire arrays and each cross-point may be functionalized with the insertion of suitable molecules [6].

The first method for the non-lithographic preparation of ultra-dense line arrays was originally proposed by Natelson et al. [7]. It is essentially based on the sequential alternate deposition of two films A and B characterized by the existence of a preferential etch for one of them (say, A). After cutting at 90° , polishing, and controlled etching of A, one eventually gets a mold that can be used as a mask for imprint lithography (IL). Actually IL is a *contact* (rather than *proximity*) lithography; what is non-lithographic is uniquely the way used for the preparation of the mask. The first practical application of this idea was provided by Melosh et al. [8] who prepared a contact mask for IL with pitch of 16 nm by growing on a

G. F. Cerofolini · D. Narducci · E. Romano (✉)
CNISM and Department of Materials Science, University
of Milano–Bicocca, Via Cozzi 53, 20125 Milano MI, Italy
e-mail: elisabetta.romano@mater.unimib.it

P. Amato
Numonyx, 20041 Agrate Brianza MI, Italy

substrate a quantum well via molecular beam epitaxy, cutting the sample perpendicularly to the surface, polishing the newly exposed surface, and etching selectively the different strata of the well.

Another route for the non-lithographic preparation of ultra-dense line arrays is the multi-spacer patterning technique (SⁿPT). This technology was developed by Cerofolini et al. [9, 10] with the goal of producing wire arrays with pitch on the nanometer length scale exploiting the already existing CMOS (complementary metal-oxide-semiconductor) IC (integrated circuit) technology only. In this way the SⁿPT may be viewed as a conservative extension of the current IC technology to the nanoscale length scale [11]. In the original formulation of SⁿPT (hereinafter referred to as ‘additive route’, SⁿPT₊) an array of $2n$ bars is directly defined onto a substrate via a sequence of n conformal depositions and anisotropic etchings. This idea is just an extension of the spacer patterning technique (SPT), conventionally used in microelectronics for the self-alignment of the gate electrode on source-and-drain regions [12]. The density limit of crossbars prepared using SⁿPT₊ are discussed in Ref. [13]: although cross-point density of 8×10^{10} could be achieved within the current technology, the overall process would however require 20 repetitions of each SPT cycle.

Multiplicative Route

Managing so many deposition-etching cycles may however be difficult and expensive. Observing that the SPT allows, starting from one seed, the preparation of *two* spacers, the above difficulty may be removed using a *multiplicative* variant (referred to as SⁿPT_×) of the multi-spacer patterning technique.

SⁿPT_× requires that each newly grown spacer is used as seed for the subsequent growth—that is possible if the original seed is etched away at the end of any cycle. In SⁿPT_× each multiplicative SPT_× cycle involves therefore the following steps:

- (i) the conformal deposition of a film on an assigned seed of high aspect ratio,
- (ii) anisotropic etching of the film down to the appearance of the original seed, and
- (iii) the selective etching of the seed.

Figure 1 sketches two SPT_× repetitions and shows that the material nature changes on going from one set of spacers to the subsequent one, so that the spacer material alternates, in our preferred embodiment, between poly-silicon and SiO₂. Since the wire material is poly-silicon, the material of the first deposited layer depends on the parity of n : if n is even, it should be in SiO₂; otherwise in poly-silicon.

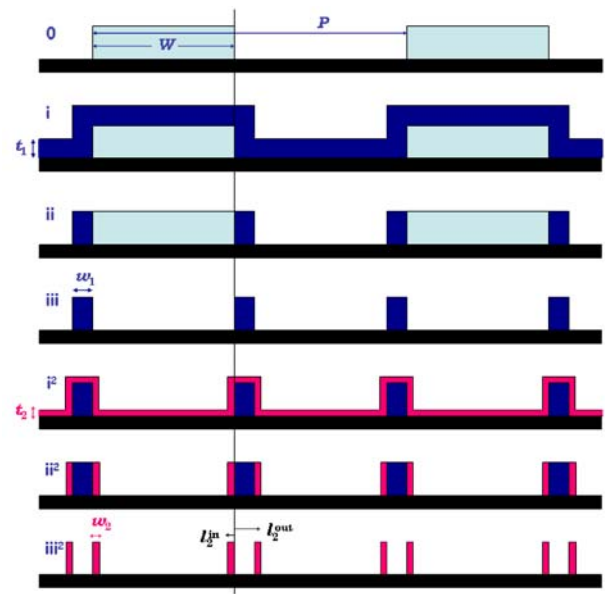


Fig. 1 Two steps for the formation of a sub-lithographic wire array starting from a lithographic seed array

The figure, however is highly idealized and does not show that, due to unavoidable side effects, the height of the spacer at a given stage is lower than that at the previous stage [13]; previous studies have shown that the spacer height t_n decreases from the height of the lithographic seed t_0 almost linearly with n ,

$$t_n = t_0 - n\tau, \quad (1)$$

with τ being the height loss per SPT_× cycle; τ depends on how accurately the technology has been set.

The first demonstrators of SⁿPT_× for the generation of gratings sub-lithographic pitch go back to more than a score of years [14]; the usefulness of this technique for the preparation of wire arrays potentially useful for biochips, instead, is much more recent [15].

Let P and W denote the lithographic pitch and wire width, respectively; P is determined by the considered lithographic technology while W may be varied almost at will controlling exposure, etching, etc. As discussed in Ref. [13], the maximum density is however achieved taking

$$P = 3W \quad (2)$$

and depositing on the bar of width w_{n-1} a conformal film of thickness s_n given by $s_n = \frac{1}{2}w_{n-1} = \frac{1}{2}s_{n-1}$, so that

$$w_n = s_n = \frac{1}{2^n}W. \quad (3)$$

While the repetition in additive way of n SPTs per (bottom and top) layers magnifies the lithographically achievable cross-point density by a factor of $(2n)^2$, the repetition in a multiplicative way gives a magnification of 2^{2n} .

This matter is discussed thoroughly in another paper [13]; rather, in this work we intend to discuss another property of S^nPT_\times —the possibility of preparing self-similar features with sub-lithographic definition.

The Multiplicative Route as a Technique for the Generation of Fractal Structures

Imagine for a moment that, in spite of the atomistic nature of matter and of the inherent technological difficulties, the multiplicative route can be repeated indefinitely. Remembering that the $(n + 1)$ -th step generates a set S_{n+1} that is nothing but the one at the n -th, S_n , at a lower scale, the sequence $\{S_0, \dots, S_n, \dots\}$ defines a fractal; it will be referred to as multi-spacer set fractal. Assuming the scaling law above [Eq. (3)], this fractal is self-similar only if the height of each spacer varies with n as 2^{-n} . Otherwise, if the structure scales only in one dimension or if its height scales with different law than in (Eq. (3)), the fractal is self-affine [16]. As mentioned above, the ‘spontaneous’ height decreases with n (Eq. (1)) renders the fractal self-affine. A self-similar fractal can be obtained at the end of process planarizing the whole structure with a resist and sputter etching in a non-selective way the composite film until the thickness is reduced to $t_0/2^n$.

It is however noted that even ignoring the technological factors, the atomistic structure of matter limits the above considerations to an interval of 1–2 orders of magnitude, ranging from few atomic layers to the lower limits of standard lithography.

Having clarified in which limits the set S_n may be considered a fractal, it is interesting to compare it with other fractal sets. The prototype of such sets, and certainly the most interesting from the speculative point of view, is certainly the Cantor middle-third excluded set. Figure 2 compares sequences of three discrete processes eventually leading to the multi-spacer fractal set S and to the Cantor set C . The comparison shows interesting analogies: Take $P = 2W$; if $w_n = \frac{1}{3}w_{n-1}$, the measure of each multi-fractal-step set coincides with that of the Cantor-step set. This implies that the multi-spacer fractal set has null measure.

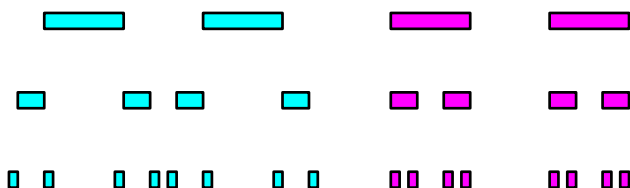


Fig. 2 Generation of the multi-spacer set (left) and of the Cantor middle-third excluded set (right)

Similarly, it can be argued that the multi-spacer set, considered as a subset of the unit interval, has the same fractal dimension as the Cantor middle-third excluded set— $\ln(2)/\ln(3)$ [16].

At each step the multi-spacer fractal set is characterized by a more uniform distribution of single intervals than the Cantor set; this makes the former more interesting for potential applications than the latter. In spite of that, trying to reproduce the Cantor set on the nanometer length scale seems of a certain interest. This is possible with existing technologies; as shown in Fig. 3, the process involves

- (C1) the lithographic definition of seed (formed, for instance, by poly-silicon) generating the Cantor set,
- (C2) its planarization (for instance, via the deposition of a low viscosity glass and its reflow upon heating),
- (C3) the etching of this film to a thickness controlled by the exposure of the original seed,
- (C4) the selective etching of the original film,
- (C5) the conformal deposition of a film of the same material as the original seed (poly-silicon, in the considered example) and of thickness equal to 1/3 of its width,
- (C6) its anisotropic etching, and
- (C7) the selective etching of the space seed (glass, in the considered example).

Although the preparation of fractal structures may appear at a first sight nothing but a mere exercise of technology stressing, in the following we discuss some of

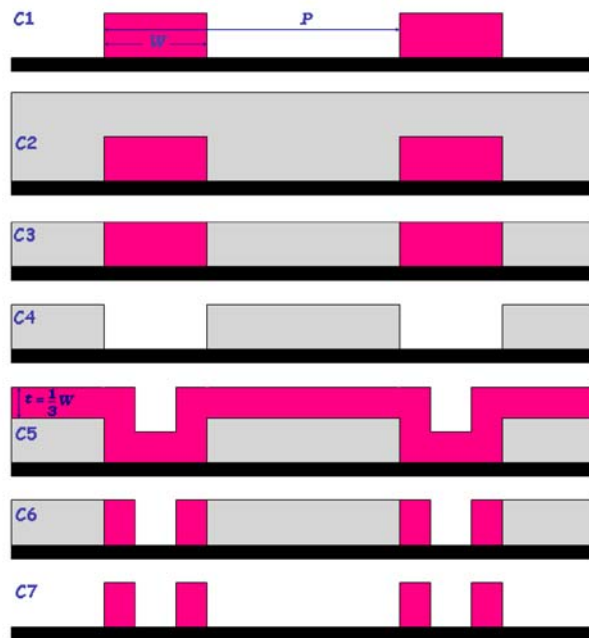


Fig. 3 A process for the generation of Cantor middle-third excluded set

their possible applications: (1) Systems biology, i.e. the study of the complex interactions in biological systems, is now overcoming the limits of molecular biology. Systems biology requires the knowledge of the cellular state at subcellular level (single constituting organelles: mitochondria, ribosomes, etc.). Sensing at this level, with space resolution in the deep sub-micrometer region, is impossible with CMOS devices, defined lithographically. Several attempts to overcome the CMOS limits are known [17, 18]; fractal technology, being able to transform a smart lithographic pattern (i.e. designed to the wanted function) in itself at a much lower scale, seems suitable for such a purpose. In particular, a matrix formed by the Cartesian product of two Cantor sets [16] would have next-to-nothing contact area, thus providing sensing with minimum perturbation. (2) Superhydrophobic surfaces may be prepared controlling roughness and surface tension of non-wetting surfaces [19, 20, 21]. Whereas surface tension is a material property, roughness can be controlled by the preparation. For instance, roughness may be imparted depositing a suitable relief on the surface. In this way, however, an amount of area is lost for other application. Although it is possible that the control of wetting properties does not require to manage geometries on the nanoscale, this loss may be minimized designing the relief in such a way as to have almost nil area (as in the example above). (3) If the S^nPT is used for the preparation of crossbar structures for molecular electronics, the functionalization with organic molecules of the cross-points can only be done after the preparation of the hosting structure. According to the analysis of Ref. [22], this requires an accurate control of the rheological and diffusion properties in a medium embedded in a domain of complex geometry. Understanding how such properties change when the size is scaled and clarifying to which extent the domain can indeed be viewed as a fractal (so allowing the analysis on fractals [23] to be used for their description) may be a key point for the actual exploitation of already producible nanometer-sized wire arrays in molecular electronics.

Discussion

Figure 4 shows in plan view a comparison between the following crossbars:

- a 2×2 crossbar obtained by crossing lithographically defined lines;
- a 16×16 crossbar obtained via S^8PT_+ starting from lithographically defined seeds separated by a distance allowing the optimal arrangement of the wire arrays;

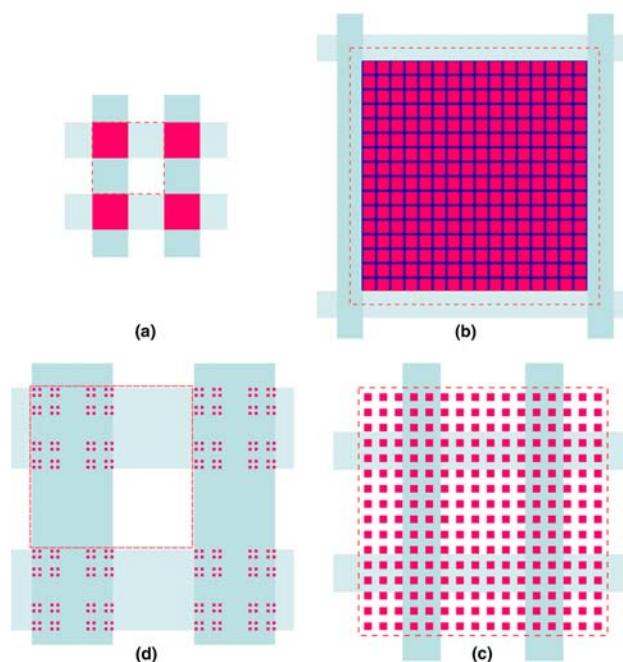


Fig. 4 Plan-view comparison of the crossbars obtained (a) crossing lithographically defined lines, (b) using the lithographically defined lines above as seeds for S^8PT_+ , (c) using the lithographically defined lines above as seeds for S^3PT_x , and (d) a Cantor middle-third excluded set using a minor variant of S^3PT_x . In each structure the square with dashed sides denotes a unit cell suitable for the complete surface tiling

- a 16×16 crossbar obtained via S^3PT_x starting from lithographically defined seeds separated by a distance satisfying Eq. (2), and
- a 16×16 crossbar obtained via S^3PT_x starting from lithographically defined seeds and arranging the process to generate the Cantor middle-third excluded set.

The figure has been drawn in the following hypotheses:

- the lithographic lines in (a) and (b) have width at the current limit for large-volume production, say $W = 65$ nm;
- the height loss τ is such that the maximum number of repetitions in the additive route is 8, and the sub-lithographic pitch is the same as reported in Refs. [9, 10]; and
- the lithographic width of (c) is chosen to allow the minimum pitch to be consistent with the one obtained with the additive route ($W = 100$ nm), in this way producing sub-lithographic wires with width (12.5 nm) that has been proved to be producible [15].

Figure 4 shows that the multiplicative route succeeds in producing crossbars with cross-point density comparable with that achieved with the additive route, however, using a remarkable smaller number of SPT repetitions. To estimate the advantage of S^nPT_x over S^nPT_+ , consider for instance

the case of the repetition of three SPT_{\times} per layer. This would produce a magnification of the lithographic cross-point density by a factor of $2^3 \times 2^3$. Taking $W = 0.1 \mu\text{m}$, after 3 SPT_{\times} repetitions the spacer width should be of 12.5 nm, with minimum separation of 25 nm. Taking into account Eq. (2), the cross-point density achievable with the repetition of $2 \times 3 SPT_{\times}$ would thus be nearly the same as that obtainable with the repetition of $2 \times 8 SPT_{+}$.

Conclusions

Some fractals (Cantor set, Peano and Koch curves, etc.) were known in mathematics well before the construction of a comprehensive theory [16]. Actually, the theory of fractals affirmed as such that only after Mandelbrot observation many physical phenomena can be described, although approximately and on a limited length scale, as fractals [24].

The usefulness of fractal algorithm is well known: assuming that human hairpins can be described, at least approximately as fractals, the use of fractal generator, rather than of the whole image, would greatly simplify storage and transmission of the corresponding image.

That real systems may be pictured as fractal set on the nanometer (and thus microscopic) length scale was first demonstrated by the analysis by Avnir, Farin and Pfeifer for the surfaces of several porous adsorbents [25, 26, 27]. In this work we have shown that the multiplicative route of the multi-spacer patterning technique allows the preparation of ordered fractals on the mesoscopic length scale.

Although at this stage we have no ideas of the possible practical applications of fractal technology, we nonetheless believe that the possibility of preparing, without the use of advanced lithography, fractal structures at the mesoscopic scale opens a virgin field of applications. The above considerations are certainly highly speculative, but not so speculative as those contained in van Gulick's paper in topochemistry [28], outlining applications currently not achievable at that time, but later demonstrated to be possible.

References

1. A.M. Stoneham, Mater. Sci. Eng. C **23**, 235 (2003)
2. M. Forshaw, R. Stadler, D. Crawley, K. Nikolic, Nanotechnology **23**, S220 (2004)
3. J.R. Heath, P.J. Kuekes, G.S. Snider, R.S. Williams, Science **280**, 1716 (1998)
4. K.K. Likharev, in *Nano and Giga Challenges in Microelectronics*, ed. by J. Greer, A. Korkin, J. Labanowsky (Elsevier, Amsterdam, 2003)
5. P.J. Kuekes, D.R. Stewart, R.S. Williams, J. Appl. Phys. **97**, 034301 (2005)
6. G.F. Cerofolini, Appl. Phys. A **86**, 31 (2007)
7. D. Natelson, R.L. Willett, K.W. West, L.N. Pfeiffer, Appl. Phys. Lett. **77**, 1991 (2000)
8. N.A. Melosh, A. Boukai, F. Diana, B. Gerardot, A. Badolato, J.R. Heath, Science **300**, 112 (2003)
9. G.F. Cerofolini, G. Arena, M. Camalleri, C. Galati, S. Reina, L. Renna, D. Mascolo, V. Nosik, Microelectr. Eng. **81**, 405 (2005)
10. G.F. Cerofolini, G. Arena, M. Camalleri, C. Galati, S. Reina, L. Renna, D. Mascolo, Nanotechnology **16**, 1040 (2005)
11. G.F. Cerofolini, Nanotechnol. E-Newslett. **7**, 5 (2005)
12. W.R. Hunter, T.C. Holloway, P.K. Chatterjee, A.F. Tasch Jr., IEEE Electron Device Lett. **2**, 4 (1981)
13. G.F. Cerofolini, P. Amato, E. Romano, Semicond. Sci. Technol. **23**, 075020 (2008)
14. D.C. Flanders, N.N. Efremow, J. Vac. Sci. Technol. B **1**, 1105 (1983)
15. Y.-K. Choi, J.S. Lee, J. Zhu, G.A. Somorjai, L.P. Lee, J. Bokor, J. Vac. Sci. Technol. **21**, 2951 (2003)
16. K. Falconer, *Fractal Geometry: Mathematical Foundations and Applications* (Wiley, New York, 2003)
17. L. Hood, J.R. Heath, M.E. Phelps, B. Lin, Science **306**, 640 (2004)
18. E. Stern, J.F. Klemic, D.A. Routenberg, P.N. Wyrenbak, D.B. Turner-Evans, A.D. Hamilton, F.A. LaVan, T.M. Fahmy, M.A. Reed, Nature **445**, 519 (2007)
19. R.N. Wenzel, Ind. Eng. Chem. **28**, 988 (1936)
20. A.B.D. Cassie, S. Baxter, Trans. Faraday Soc. **40**, 546 (1944)
21. A. Tuteja, W. Choi, M. Ma, J.M. Mabry, S.A. Mazzella, G.C. Rutledge, G.H. McKinley, R.E. Cohen, Science **318**, 1618 (2007)
22. G.F. Cerofolini, V. Casuscelli, A. Cimmino, A. Di Matteo, V. Di Palma, D. Mascolo, E. Romanelli, M.V. Volpe, E. Romano, Semicond. Sci. Technol. **22**, 1053 (2007)
23. J. Kigami, *Analysis on Fractals* (Cambridge Univ. Press, Cambridge, 2001)
24. B.B. Mandelbrot, *The Fractal Geometry of Nature* (Freeman, New York, 1982)
25. P. Pfeifer, D. Avnir, J. Chem. Phys. **79**, 3558 (1983)
26. D. Avnir, D. Farin, P. Pfeifer, J. Chem. Phys. **79**, 3566 (1983)
27. D. Avnir, D. Farin, P. Pfeifer, Nature **308**, 261 (1984)
28. N. Van Gulick, New J. Chem. **17**, 619 (1993)